Broj rada: R4-11
DOI:10.46793/CIRED2026.R4-11 156

UTICAJ FOTONAPONSKIH SISTEMA SA BATERIJSKIM SKLADIŠTENJEM ENERGIJE, VOĐENIH ENERGETSKOM ARBITRAŽOM, NA RAD DISTRIBUTIVNE MREŽE

IMPACT OF ARBITRAGE-DRIVEN PHOTOVOLTAIC–BATTERY SYSTEMS ON DISTRIBUTION NETWORK OPERATION

Goran VELJANOVSKI*, Faculty of Technical Sciences, N. Macedonia
Faruk ŠEHIĆ, Elektroprivreda Bosne i Hercegovine, Bosna i Hercegovina
Pande POPOVSKI, Faculty of Technical Sciences, N. Macedonia
Nikolče ACEVSKI, Faculty of Technical Sciences, N. Macedonia
Elena KOTEVKSA, Faculty of Technical Sciences, N. Macedonia
Blagoja ARAPINOSKI, Faculty of Technical Sciences, N. Macedonia
Mitko KOSTOV, Faculty of Technical Sciences, N. Macedonia
Metodija ATANASOVSKI, Faculty of Technical Sciences, N. Macedonia

KRATAK SADRŽAJ

Sve veće učešće promenljivih obnovljivih izvora energije značajno je preoblikovalo profile cena električne energije u savremenim elektroenergetskim sistemima. Na mnogim veleprodajnim tržištima, klasična cenovna „duck curve“ kriva postepeno se transformiše u izraženu dolinu cena tokom sredine dana, prvenstveno usled masovne integracije fotonaponske proizvodnje. Fotonaponska tehnologija postala je jedan od najrasprostranjenijih obnovljivih izvora energije na globalnom nivou, zahvaljujući modularnosti, opadajućim investicionim troškovima i povoljnim politikama podrške. Međutim, proizvodni profil fotonaponskih elektrana često je slabo usklađen sa profilima cena električne energije. Ova rastuća neusklađenost dovodi u pitanje ekonomsku isplativost investicija zasnovanih isključivo na fotonaponskim sistemima i izlaže investitore povećanim tržišnim rizicima. Kao odgovor na to, baterijski sistemi za skladištenje energije sve se češće integrišu s fotonaponskim elektranama kako bi se omogućila energetska arbitraža i povećali prihodi. Prebacivanjem energije iz perioda niskih cijena u intervale s višim cijenama, PV-BESS sistemi predstavljaju obećavajući način za ponovno uspostavljanje i unapređenje profitabilnosti. Istovremeno, masovna primjena ovakvih hibridnih sistema uvodi nove tehničke i operativne izazove u distributivnoj mreži, pri čemu regulacija napona, opterećenje vodova, promjene smjera tokova snage i upravljanje zagušenjima postaju ključni izazovi. U ovom radu se istražuje uticaj fotonaponskih elektrana opremljenih baterijskim sistemima za skladištenje energije na rad i performanse distributivnih mreža. Analiza je usmerena na to kako strategije punjenja i pražnjenja vođene energetskom arbitražom utiču na mrežna ograničenja, naponske profile i tokove snage. Rezultati ukazuju na kompromis između tržišno zasnovane profitabilnosti i sigurnosti rada distributivne mreže. Zbog toga je neophodno eksplicitno uvažiti mrežna ograničenja kako bi se ostvarile ekonomske koristi od PV-BESS sistema uz očuvanje pouzdanog rada mreže.

Ključne reči: baterijski sistemi za skladištenje energije, distributivne mreže, fotonaponski elektrana

* Goran Veljanovski goran.veljanovski@uklo.edu.mk

ABSTRACT

The increasing penetration of variable renewable energy sources has significantly reshaped electricity price profiles in modern power systems. In many wholesale markets, the classical price “duck curve” is gradually evolving toward a pronounced mid-day price valley, driven primarily by the large-scale integration of photovoltaic generation. PV technology has become the most widely deployed renewable energy source worldwide due to its modularity, declining investment costs, and favorable policy support. However, the generation profile of PV plants is often poorly aligned with electricity price profiles. This growing mismatch challenges the economic feasibility of PV-only investments and exposes investors to increasing market risks. As a response, battery energy storage systems are increasingly being coupled with PV plants to enable energy arbitrage to improve revenue streams. By shifting energy from low-price periods to high-price intervals, PV-BESS systems offer a promising pathway to restore and enhance profitability. At the same time, the large-scale deployment of such hybrid systems introduces new technical and operational challenges at the distribution network level, where voltage regulation, line loading, power flow reversals, and congestion management become critical concerns.This paper investigates the impact of PV plants equipped with BESS on the operation and performance of distribution networks. The analysis focuses on how energy arbitrage-driven charging and discharging strategies influence network constraints, voltage profiles, and power flows. The results show a trade-off between market-based profitability and distribution network security, highlighting that network constraints must be explicitly considered to achieve economic benefits from PV–BESS systems while maintaining reliable network operation.

Keywords: battery energy storage systems, distribution network, photovoltaic systems

1. INTRODUCTION

The increasing penetration of solar PV in electricity markets has led to a decline in wholesale electricity prices during periods of high generation. This is mainly due to the zero marginal cost of PV production, which replaces more expensive generation units through the merit-order effect [1]. Several studies have shown that as the share of PV increases, the average price received by PV producers decreases, and this effect becomes stronger at higher penetration levels [2]. As a result, the revenues of PV systems decrease over time, reducing their economic attractiveness and making new investments less appealing [3]. In many cases, this reduction in profitability has made the integration of battery energy storage systems (BESS) necessary in order to maintain acceptable economic performance [4]. Among the different ways BESS can generate revenue, energy arbitrage is considered one of the most profitable strategies [5]. Several studies have shown that optimization methods, such as mixed-integer linear programming (MILP), can be used to schedule battery operation in day-ahead markets in a way that maximizes profit over time [6].

However, when BESS units operate independently and aim only to maximize their own profit, their combined effect on the distribution network (DN) can be negative. Reference [7] showed that poorly sized or improperly operated BESS can lead to voltage problems and overloading of network components, depending on how the batteries are used. Similarly, [8] found that PV systems with BESS operating under individual control strategies do not necessarily improve network performance and may even worsen voltage conditions in some parts of the network. When many BESS units discharge at the same time during high-price evening hours, they inject

power simultaneously into the network, which can increase voltages and network losses [9]. On the other hand, when they charge at the same time during low-price periods, especially if charging from the grid is allowed, they can create new demand peaks that may overload lines and transformers [10]. The authors in [11] showed that under such uncoordinated operation, a large share of distribution transformers may need to be upgraded in the future due to increased loading. At the feeder level, battery charging has also been shown to increase power losses because of higher current flows [9,] [12]. In addition, BESS units operating based only on price signals tend to behave in a similar way, creating synchronized charging and discharging patterns across the network. This leads to new peaks and fluctuations in power flows that the distribution system was not originally designed to handle [13]. As PV penetration approaches the hosting capacity of the network and more BESS units are added, these effects are expected to become even more significant, since both the amount of power and the level of synchronization between units increase [7], [8].

In this context, the aim of this paper is to analyze the impact of PV–BESS systems on the operation of a real DN. First, the existing network with currently installed PV systems is considered, after which BESS are added to each PV installation and operated under energy arbitrage strategies. Subsequently, the hosting capacity of the network is determined, and additional PV units are installed at selected nodes up to this limit, with corresponding BESS units integrated as well. The study evaluates how these scenarios influence key network performance indicators, including voltage profiles, line loading, and power flow patterns. Particular attention is given to identifying the conditions and time periods under which operational constraints are violated, in order to assess the severity and timing of potential network issues arising from large-scale PV–BESS deployment.

The remainder of this paper is organized as follows. Section 2 describes the operation of BESS under energy arbitrage strategies, outlines the methodology for hosting capacity assessment, and presents the data used in the study. Section 3 presents the obtained results and provides a discussion of their impact on DN performance. Finally, Section 4 summarizes the main conclusions of the paper.

2. METHODOLOGY AND DATA

2.1 BESS operation

In order to analyze the impact of BESS on the operation of the DN, a battery is added to each existing PV installation. The BESS is operated under an energy arbitrage strategy, where charging and discharging decisions are driven by electricity price variations with the objective of maximizing daily revenue. In this way, a new net generation profile of the hybrid PV–BESS system is obtained, which is subsequently used as an input for the DN analysis. The optimization problem is formulated to maximize the net profit over the scheduling horizon as follows:

$$\max \sum_{t=0}^{T} \left(\lambda_t^{\text{sell}} P_t^{\text{ex}} - \lambda_t^{\text{buy}} P_t^{\text{im}} \right) \tag{1}$$

where λ_t^{sell} is the selling price of electricity, λ_t^{buy} the buying price of electricity, and P_t^{ex} and P_t^{im} denote the exported and imported power at time step t, respectively, defined as:

$$P_t^{\text{export}} = P_t^{\text{PV}} + P_t^{\text{dis}} - P_t^{\text{ch}} \tag{2}$$

$$P_t^{\text{import}} = P_t^{\text{ch}} \tag{3}$$

where P_t^{PV} is the PV generation, and P_t^{ch} and P_t^{dis} denote the charging and discharging power of the BESS at time step t, respectively.

The operation of the battery is subject to the following constraints. The state of charge (SoC) dynamics are described by:

$$SoC_{t+1} = SoC_t + \eta^{\text{ch}} P_t^{\text{ch}} - \frac{1}{\eta^{\text{dis}}} P_t^{\text{dis}}, t = 0,\ldots,T \tag{4}$$

where η^{ch} and η^{dis} denote the charging and discharging efficiency, respectively. The SoC of the battery at each time step is bounded by:

$$SoC^{\min} \le SoC_t \le SoC^{\max}, \quad t = 0,\ldots,T \tag{5}$$

The charging and discharging powers are limited by:

$$\begin{aligned} 0 \le P_t^{\text{ch}} \le P^{\text{ch,max}}, \quad t = 0,\ldots,T \\ 0 \le P_t^{\text{dis}} \le P^{\text{dis,max}}, \quad t = 0,\ldots,T \end{aligned} \tag{6}$$

To prevent simultaneous charging and discharging, a binary variable y_t is introduced:

$$y_t = \begin{cases} 1, & \text{if the battery is charging} \\ 0, & \text{if the battery is discharging} \end{cases} \tag{7}$$

which leads to the following constraints:

$$\begin{aligned} P_t^{\text{ch}} \le y_t \cdot P^{\text{ch,max}}, \quad t = 0,\ldots,T \\ P_t^{\text{dis}} \le (1 - y_t) \cdot P^{\text{dis,max}}, \quad t = 0,\ldots,T \end{aligned} \tag{8}$$

In the case where the BESS is restricted to charging only from the PV plant, the charging power is limited by the available PV output, and no energy is imported from the grid. This is enforced through the following constraints:

$$P_t^{\text{ch}} \le P_t^{\text{PV}}, \quad P_t^{\text{import}} = 0, \quad t = 0,\ldots,T \tag{9}$$

The optimization problem is formulated as a mixed-integer linear programming (MILP) model, ensuring a physically feasible operation of the BESS while maximizing economic performance. The resulting hybrid PV–BESS power profile, expressed through P_t^{ex}, is used to evaluate the impact on distribution network performance.

2.2 Hosting capacity

The method for determining the hosting capacity is based on the approach presented in [14]. The objective of this method is to determine the maximum amount of distributed generation (DG) that can be integrated into a distribution network without violating operational constraints, i.e. voltage limits and line loading. Based on a load flow analysis, and given the branch impedances and nodal loads, the complex power flows and nodal voltages at each node can be determined.

When a DG unit is connected at node *i*, and assuming constant load conditions, part of the local demand is supplied by the DG, while the excess generation is transferred toward electrically nearby nodes and ultimately toward the reference (slack) bus. As a result, the power flow in the branches between the DG location and the reference bus is reduced, as shown on figure 1. The power flow through each branch $\underline{S}_j^N$ after DG integration at node I can be calculated as:

$$\underline{S}_j^N = \begin{cases} \underline{S}_j & if\ j\ is\ not\ incident\ to\ i \\ \underline{S}_j - \underline{S}_{DGi} & otherwise \end{cases} \tag{10}$$

In a scenario with multiple DG, the power flow through each branch can be calculated as:

$$\underline{\mathbf{S}}_j^N = \underline{\mathbf{S}}_j - \mathbf{I} \cdot \underline{\mathbf{S}}_{DG} \tag{11}$$

where $\underline{\mathbf{S}}_j^N$ is a vector of the power flow through each branch after DG integration, $\underline{\mathbf{S}}_j$ is a vector of the power flow through each branch before DG integration, $\underline{\mathbf{S}}_{DG}$ is the complex power generated from the DGs at each node, and $\mathbf{I}$ is a (0, 1) matrix with dimension no. nodes x no. nodes, and is formulated as:

$$\mathbf{I} = \begin{cases} 1\ if\ branch\ j\ is\ incident\ to\ node\ i \\ 0 \qquad\qquad otherwise \end{cases} \tag{12}$$

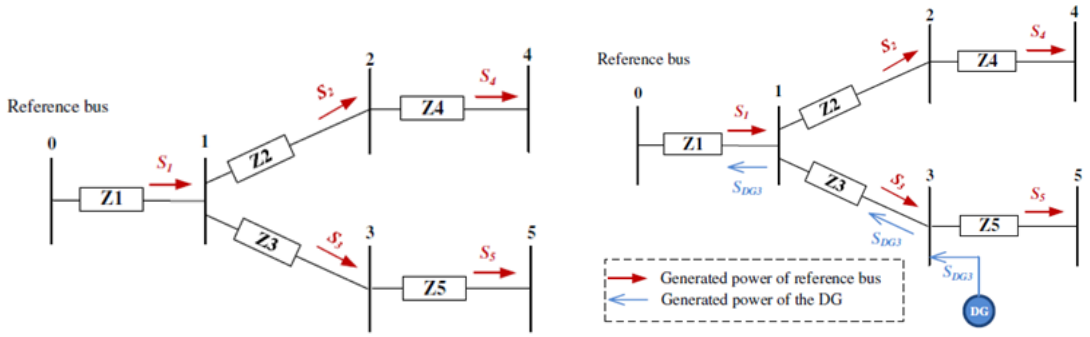
The change in loading of lines will also change the voltages of the nodes. In a radial medium voltage DN, the voltage drop can be calculated as:

$$\Delta v_{j\%} = \frac{100}{Un^2}(P_j R_j - Q_j X_j) \tag{13}$$

After integrating the DG, the new voltage v_j^N can be calculated as:

$$v_j^N = v_0 - \frac{100}{Un^2}\sum_{i\in\mathbf{B}} P_i^N R_i - Q_i^N X_i = v_0 - \frac{100}{Un^2}\sum_{i\in\mathbf{B}} (P_i - \mathbf{I}_{ji}P_{DG})R_i - (Q_i - \mathbf{I}_{ji}Q_{DG})X_i =$$

$$= v_0 - \frac{100}{Un^2}\sum_{i\in\mathbf{B}} P_i R_i - Q_i X_i + \frac{100}{Un^2}\sum_{i\in\mathbf{B}} \mathbf{I}_{ji}P_{DG}R_i - \mathbf{I}_{ji}Q_{DG}X_i = v_j + \frac{100}{Un^2}\sum_{i\in\mathbf{B}} \mathbf{I}_{ji}P_{DG}R_i - \mathbf{I}_{ji}Q_{DG}X_i \tag{14}$$



(a) (b)

Figure 1 – Load flows
(a) before connecting DG; (b) after connecting DG, izvor: [14]

where **B** is a vector containing the branches that are incident to node *j*, and $\mathbf{I}_{ji}$ is the value of the *j*-th row and *i*-th column of $\mathbf{I}$.
In a distribution network with multiple DGs, the voltage v_j^N at each node can be calculated as:

$$\mathbf{v}^N = \mathbf{v} + \frac{100}{Un^2}\left[\mathrm{Re}\{\underline{\mathbf{Z}}\}\cdot(\mathbf{I}\cdot\mathrm{Re}\{\underline{\mathbf{S}}_{DG}\}) - \mathrm{Im}\{\underline{\mathbf{Z}}\}\cdot(\mathbf{I}\cdot\mathrm{Im}\{\underline{\mathbf{S}}_{DG}\})\right] \tag{15}$$

Now, the loading at branch j can be calculated as following:

$$I_j = \frac{S_j}{\sqrt{3}\cdot\frac{U_n}{100}v_j} \tag{16}$$

The hosting capacity is determined as the maximum DG capacity that satisfies:

$$\begin{aligned} v^{\min} \le v_j \le v^{\max}, \ \forall j \\ I_k \le 1, \ \forall k \end{aligned} \tag{17}$$

2.3 Data

In order to analyze the impact of BESS integration on DN operation, a real radial 10 kV DN is considered, consisting of 56 nodes, as illustrated in figure 2. The network includes 26 medium-to-low voltage (MV/LV) transformers supplying downstream low-voltage consumers. In addition, four PV plants are connected at different nodes of the network. The installed capacities and connection points of these PV units are summarized in Table 1.

The network is modeled based on actual line parameters, transformer data, and load profiles, and represents a typical medium-voltage radial feeder. The slack bus is located at the primary substation, which connects the DN to the upstream transmission system.

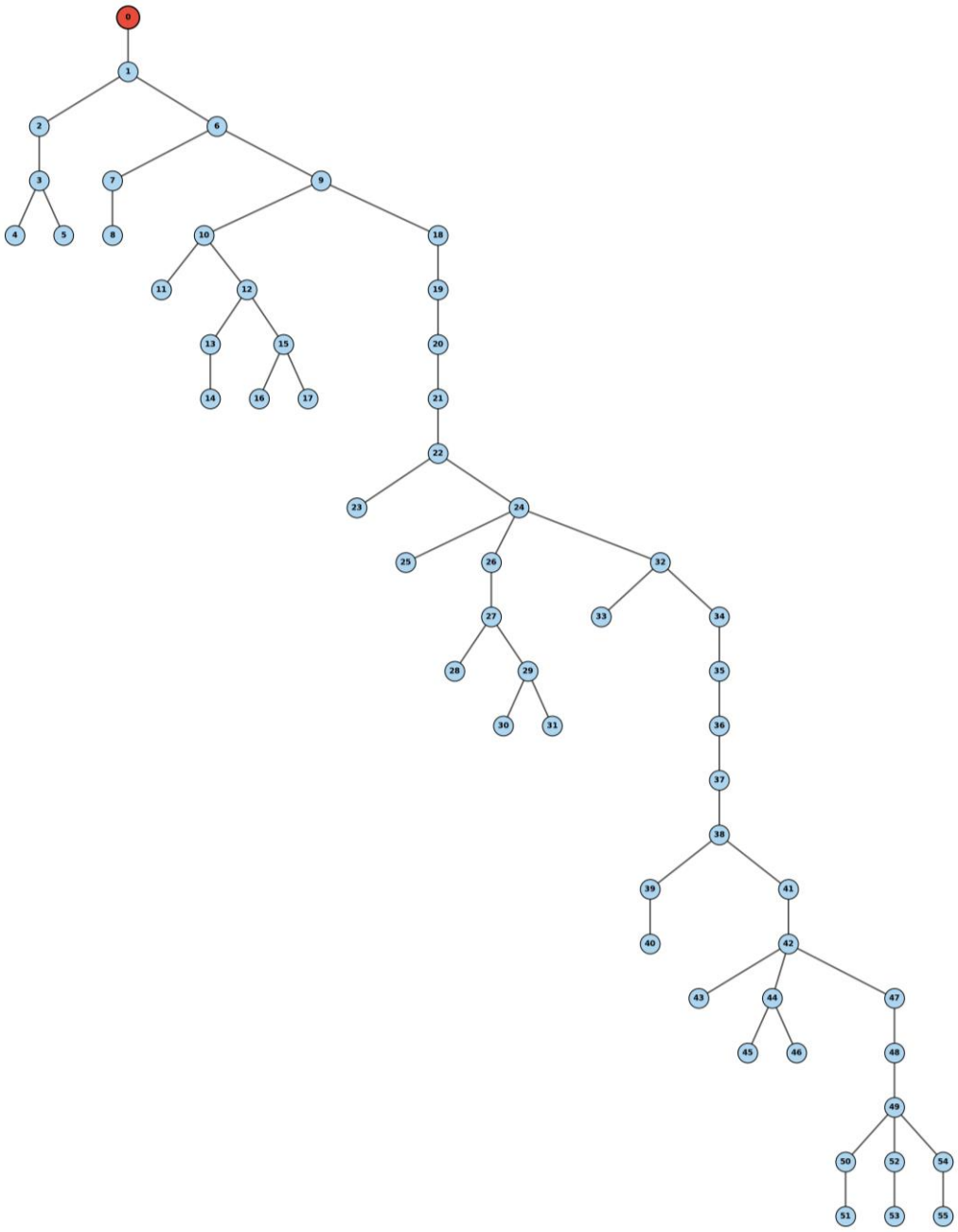


Figure 2 – Analyzed DN

Tabela I – Connected PV plants to the DN

Node to which the PV is connected	Installed capacity [kWp]
11	15
43	33
33	800
12	100

The operation of the DN is evaluated through power flow simulations with a 15-minute resolution over a one-year period. Five scenarios are considered in order to assess the impact of PV and BESS integration. Scenario 1 represents the current network configuration with the existing PV installations. In Scenario 2, a BESS is added to each PV plant, with power equal to the installed PV capacity, and the battery is restricted to charging only from local PV generation. In Scenario 3, the same PV–BESS configuration is considered, but the batteries are allowed to charge both from PV generation and from the grid. Subsequently, the hosting capacity of the network is determined, and additional PV units are installed at selected nodes up to this limit. Based on this expanded configuration, three additional scenarios are analyzed. Scenario 4 represents the network with PV installations increased up to the hosting capacity limit, without the integration of BESS. Scenario 5 considers PV–BESS systems where charging is restricted to PV generation only, while Scenario 6 allows charging from both PV and the grid. For all scenarios, the impact on voltage profiles, line loading, and power flow patterns is evaluated in order to identify potential operational constraints and their temporal occurrence.

3. RESULTS AND DISCUSION

The optimization problem formulated as a MILP model was solved using the solver [15] integrated within the programming language [16]. Time-series power flow simulations were performed in [17] over a one-year period, from 02.07.2024 to 02.07.2025, with a temporal resolution of 15 minutes. Electricity market prices for the same period were obtained from [18]. Since the available price data had an hourly resolution, the values were converted to 15-minute intervals by assigning the same hourly electricity price to each of the four corresponding 15-minute time steps within the hour. The selling price of electricity was modeled as the market price obtained from [18] reduced by 7% and additionally decreased by 2 €/MWh, in order to account for market-related fees and transaction costs. The buying price of electricity was determined as the market price from [18] increased by 10%. The proposed methodology was applied to all six analyzed scenarios, and the obtained results are presented and discussed in the following section.

Results from Scenario 1

Figures 3–6 and Table II present the obtained results for Scenario 1, representing the current operation of the analyzed DN with the existing PV installations. As shown in Figure 3, all nodal voltages remain within the admissible operating limits during the analyzed period. The minimum recorded voltage is 95.87% at node 53, while the maximum voltage reaches 108.43% at node 1. The voltage duration curve shown in Figure 4 confirms that no voltage violations occur throughout the year. This indicates that the existing PV penetration level does not introduce significant voltage regulation problems in the analyzed network. The line loading results presented in Figures 5 and 6 show that the maximum loading reaches 58.17%, occurring on line 1. No thermal overloads are observed during the analyzed period, indicating that the current network configuration operates well below its thermal limits. The annual active energy losses for Scenario 1 amount to 147.41 MWh, representing the reference case against which the remaining scenarios are compared.

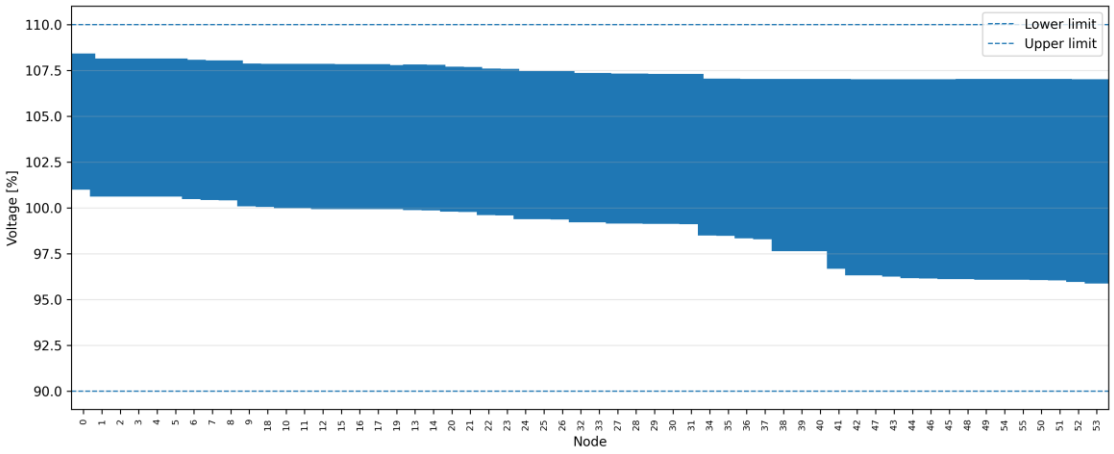


Figure 3 – Voltage range per node for Scenario 1

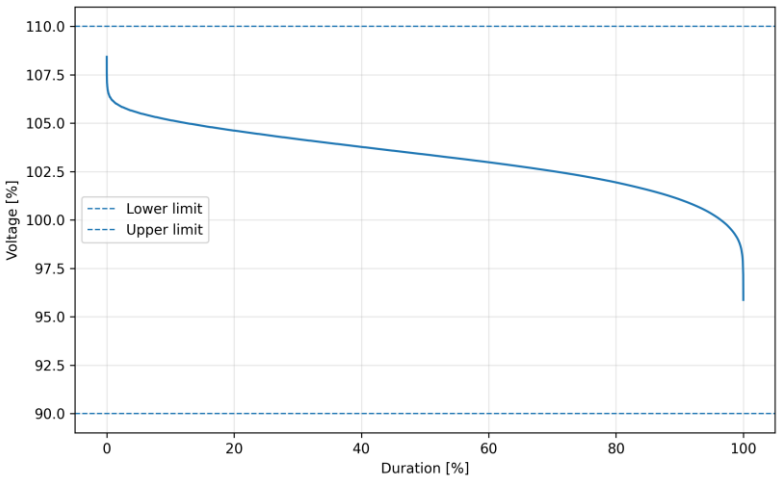


Figure 4 – Voltage duration curve for Scenario 1

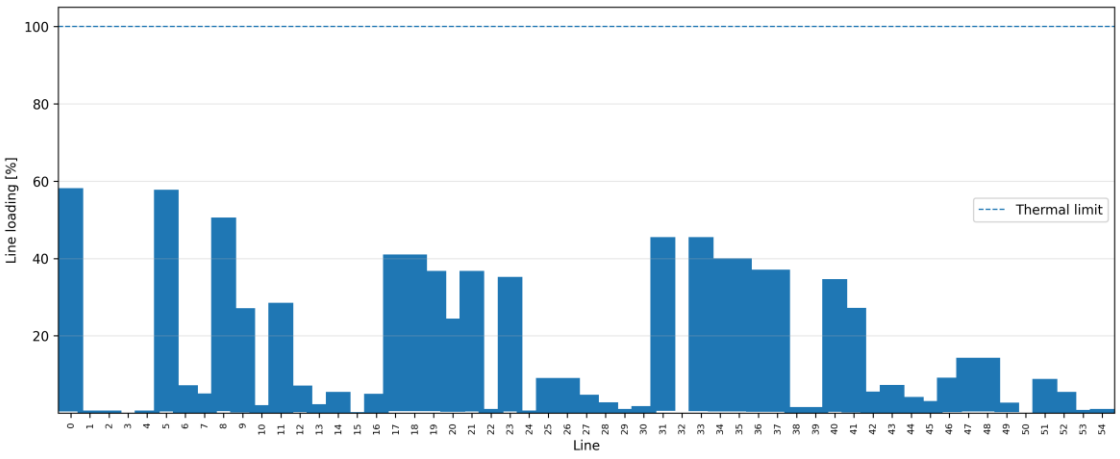


Figure 5 – Line loading range per line for Scenario 1

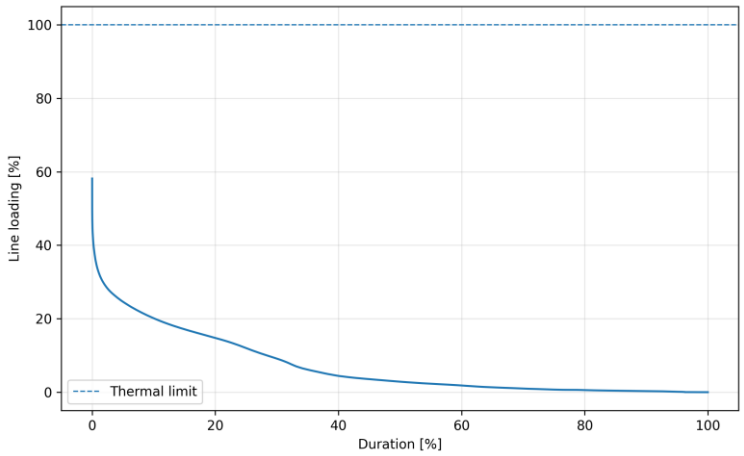


Figure 6 – Line loading duration curve for Scenario 1

Tabela II – Statistics for Scenario 1

Metric	Value	Critical element
Minimum voltage [%]	95.866	53
Maximum voltage [%]	108.4264	1
Maximum line loading [%]	58.169397	1
Nodes with undervoltage	/	/
Nodes with overvoltage	/	/
Lines with overload	/	/
Total hours below voltage limit [h]	/	/
Total hours above voltage limit [h]	/	/
Total hours above loading limit [h]	/	/
Annual active energy losses [MWh]	147.41	/

Results from Scenario 2

Figures 7–10 and Table III present the obtained results for Scenario 2, in which a BESS is added to each existing PV installation and restricted to charging only from local PV generation. Compared to Scenario 1, only minor changes in the voltage profiles can be observed. As shown in Figure 7 and summarized in Table III, the minimum and maximum voltages remain identical to those obtained in Scenario 1, while the voltage duration curve presented in Figure 8 confirms that no voltage violations occur throughout the year. Similarly, the impact on line loading remains limited. The maximum line loading shown in Figure 9 increases only slightly from 58.17% to 58.76%, while Figure 10 confirms that no thermal overloads occur during the analyzed period. The annual active energy losses increase marginally to 150.22 MWh, as shown in Table III. These results indicate that when BESS charging is restricted to local PV generation, the impact of the batteries on DN operation remains relatively small under the current PV penetration level.

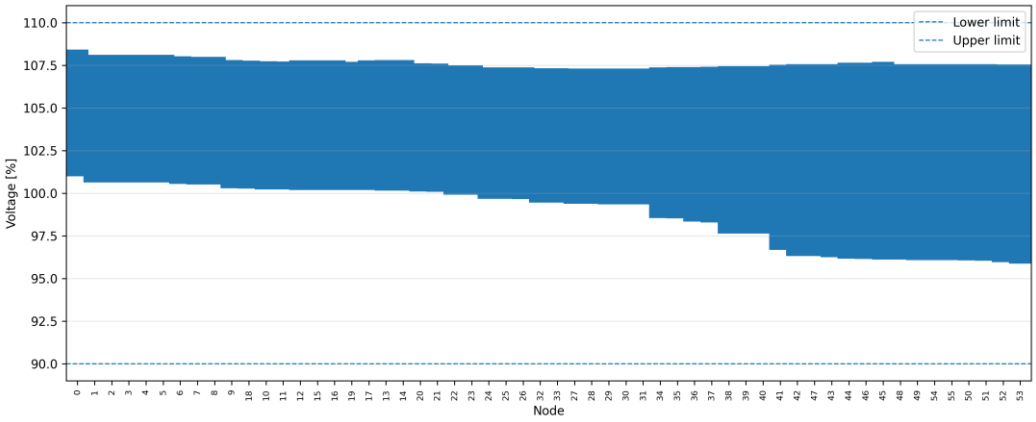


Figure 3 – Voltage range per node for Scenario 2

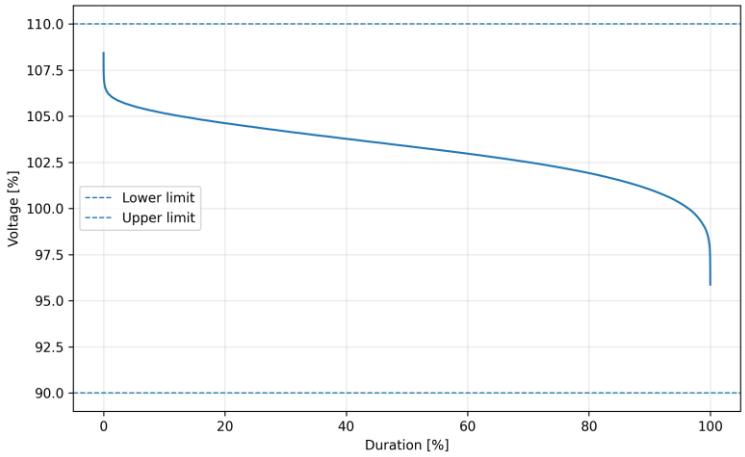


Figure 8 – Voltage duration curve for Scenario 2

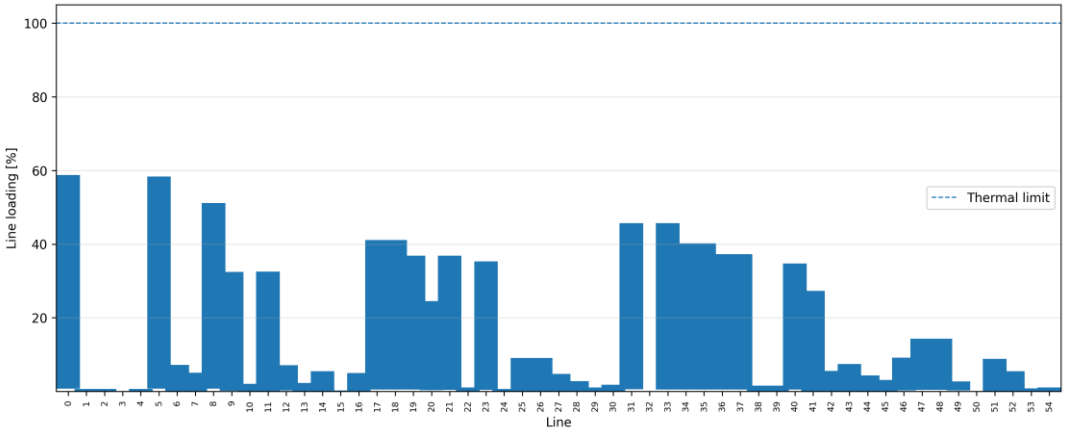


Figure 9 – Line loading range per line for Scenario 2

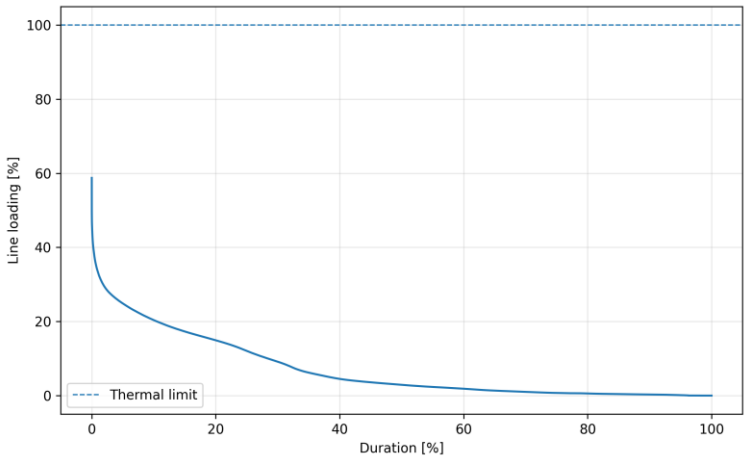


Figure 10 – Line loading duration curve for Scenario 2

Tabela III – Statistics for Scenario 2

Metric	Value	Critical element
Minimum voltage [%]	95.866	53
Maximum voltage [%]	108.4264	1
Maximum line loading [%]	58.76369	1
Nodes with undervoltage	/	/
Nodes with overvoltage	/	/
Lines with overload	/	/
Total hours below voltage limit [h]	/	/
Total hours above voltage limit [h]	/	/
Total hours above loading limit [h]	/	/
Annual active energy losses [MWh]	150.22	/

Results from Scenario 3

Figures 11–14 and Table IV present the results obtained for Scenario 3, where the BESS units are additionally allowed to charge from the grid. In comparison with Scenario 2, the voltage profiles remain relatively similar, as shown in Figure 11, while the voltage duration curve in Figure 12 confirms that no voltage violations occur. However, a noticeable increase in network loading can be observed. As presented in Figure 13 and summarized in Table IV, the maximum line loading increases to 72.80%, while the annual active energy losses rise to 169.25 MWh. Figure 14 further shows that the duration of high loading conditions becomes significantly larger compared to the previous scenarios, although no thermal limits are exceeded. This behavior is primarily caused by the simultaneous charging of multiple BESS units during low-price periods, resulting in increased demand peaks in the network.

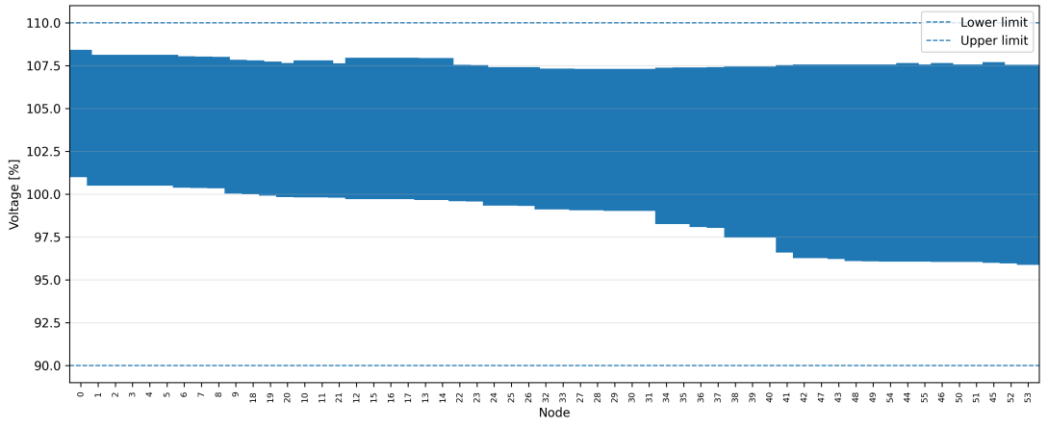


Figure 11 – Voltage range per node for Scenario 3

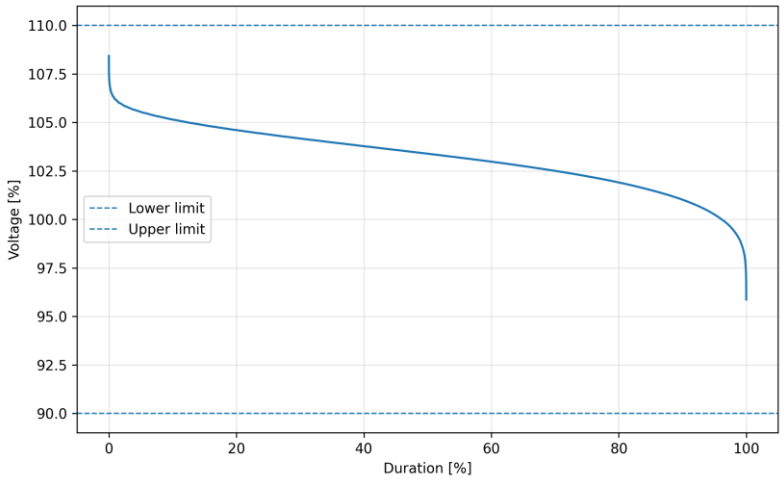


Figure 12 – Voltage duration curve for Scenario 3

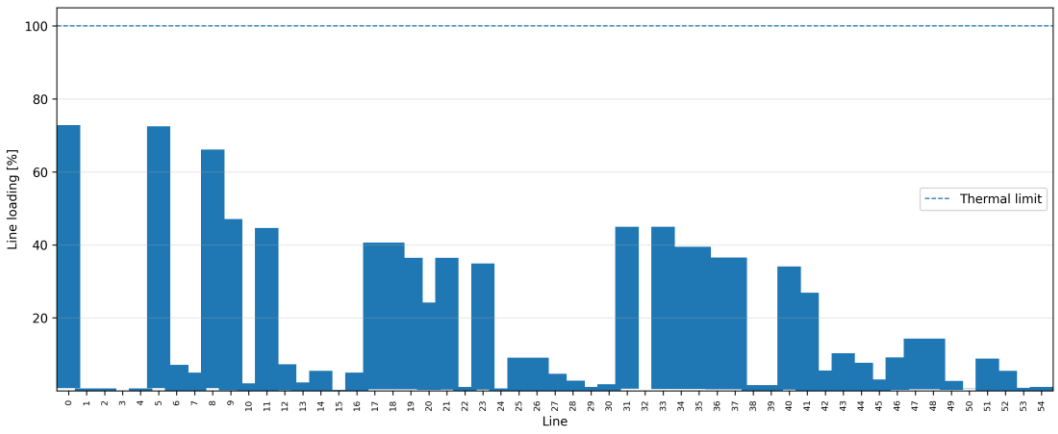


Figure 13 – Line loading range per line for Scenario 3

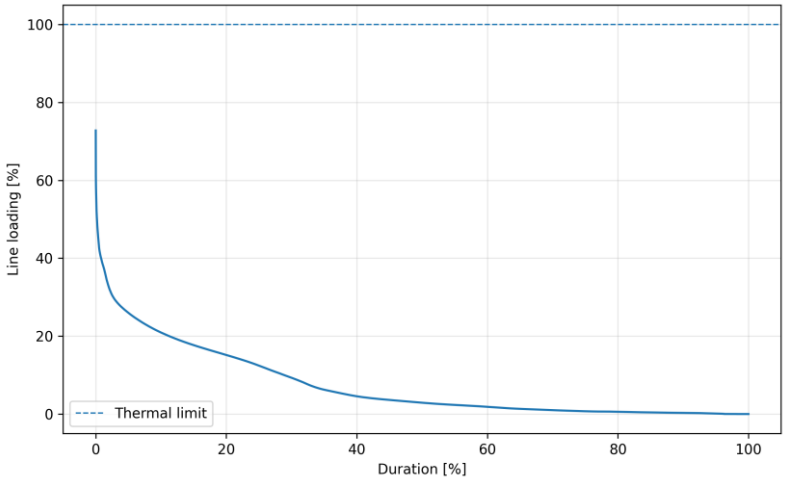


Figure 14 – Line loading duration curve for Scenario 3

Tabela VI – Statistics for Scenario 3

Metric	Value	Critical element
Minimum voltage [%]	95.866	53
Maximum voltage [%]	108.4264	1
Maximum line loading [%]	72.796	1
Nodes with undervoltage	/	/
Nodes with overvoltage	/	/
Lines with overload	/	/
Total hours below voltage limit [h]	/	/
Total hours above voltage limit [h]	/	/
Total hours above loading limit [h]	/	/
Annual active energy losses [MWh]	169.25	/

Results from Scenario 4

Figures 15–18 and Table V present the obtained results for Scenario 4, representing the network operating at the calculated hosting capacity limit without BESS integration. Due to the substantially increased PV penetration, significantly higher voltages and line loadings are observed compared to the previous scenarios. As shown in Figure 15 and summarized in Table V, the maximum voltage reaches 109.62% at node 28, approaching the upper admissible voltage limit. The voltage duration curve presented in Figure 16 shows that the network still operates without voltage violations during the analyzed year. Similarly, the line loading range shown in Figure 17 indicates that the maximum loading increases to 96.70% on line 8, while Figure 18 confirms that no thermal overloads occur. These results demonstrate that the calculated hosting capacity corresponds to the maximum PV penetration level at which the network can still operate within its operational constraints.

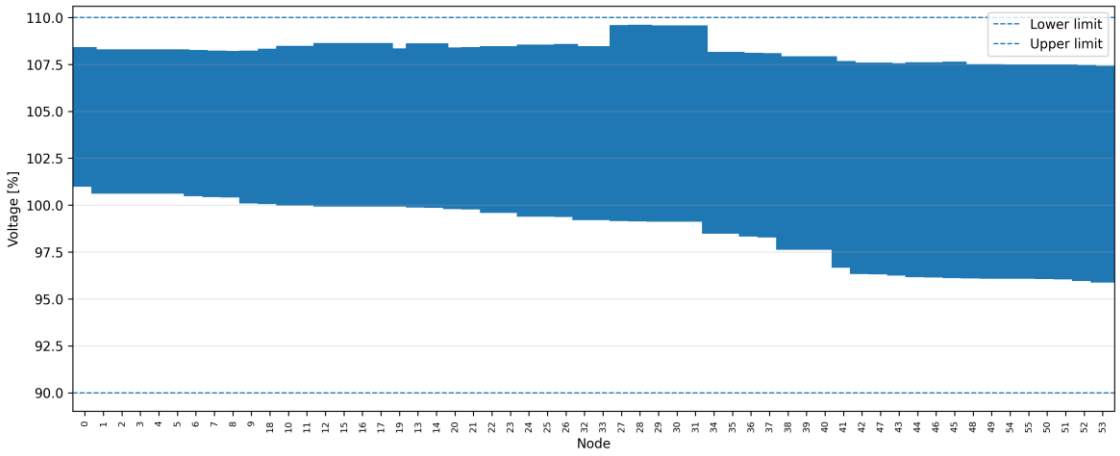


Figure 15 – Voltage range per node for Scenario 4

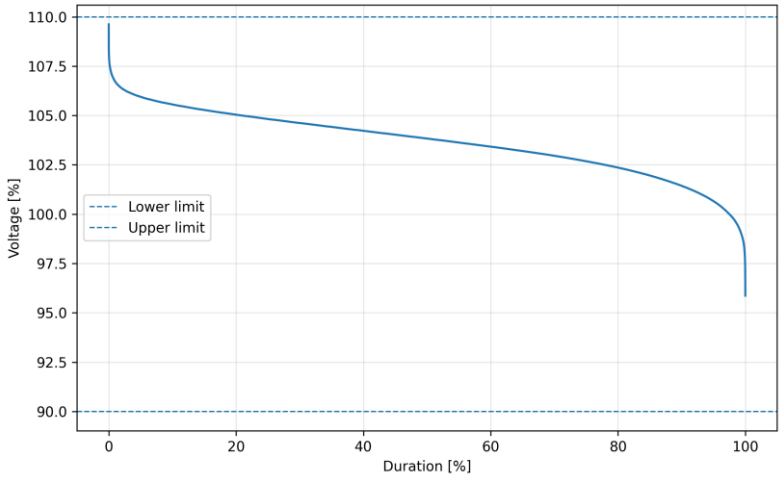


Figure 16 – Voltage duration curve for Scenario 4

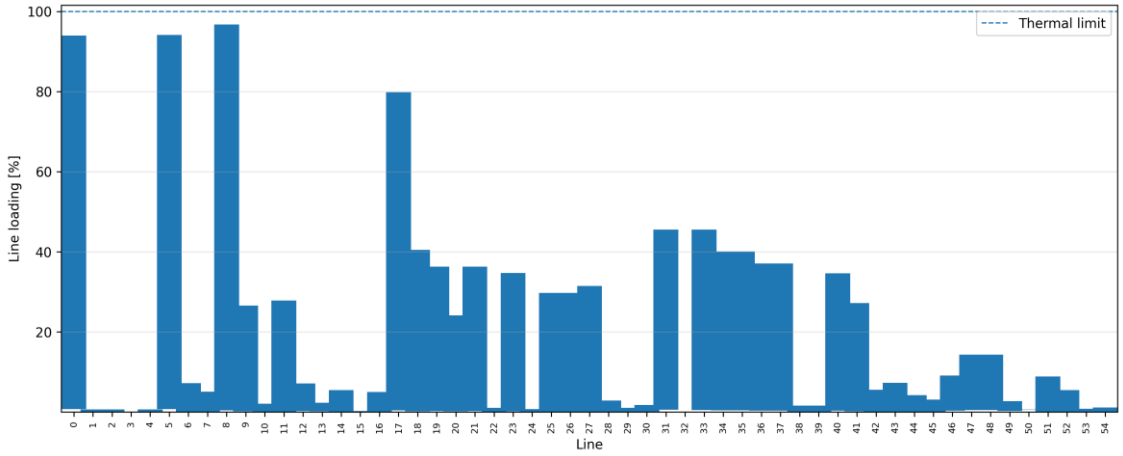


Figure 17 – Line loading range per line for Scenario 4

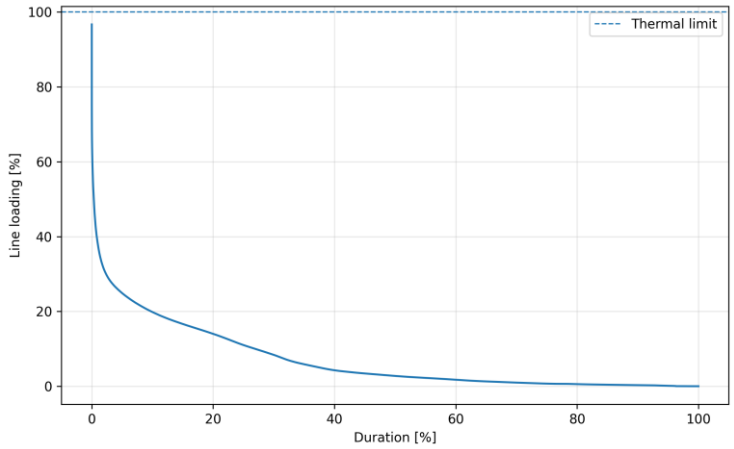


Figure 18 – Line loading duration curve for Scenario 4

Tabela V – Statistics for Scenario 4

Metric	Value	Critical element
Minimum voltage [%]	95.866	53
Maximum voltage [%]	109.6192	28
Maximum line loading [%]	96.69552	8
Nodes with undervoltage	/	/
Nodes with overvoltage	/	/
Lines with overload	/	/
Total hours below voltage limit [h]	/	/
Total hours above voltage limit [h]	/	/
Total hours above loading limit [h]	/	/
Annual active energy losses [MWh]	160.76	/

Results from Scenario 5

Figures 19–22 and Table VI present the results for Scenario 5, where BESS units are integrated into the HC level and restricted to charging only from local PV generation. In this case, the first operational constraint violations appear in the analyzed DN. As shown in Figure 19 and summarized in Table VI, the maximum voltage increases to 111.59%, resulting in overvoltage occurrences at 44 nodes. According to the voltage duration curve shown in Figure 20, the total duration of overvoltage conditions reaches 42.5 hours throughout the year. At the same time, the maximum line loading shown in Figure 21 increases to 112.93%, resulting in overloads on three lines. Figure 22 further indicates that the total duration of thermal overloads reaches 15.75 hours annually. In addition, the annual active energy losses increase to 200.35 MWh, as shown in Table VI. These results indicate that under high PV penetration conditions, even BESS systems restricted to charging only from local PV generation can introduce significant operational challenges due to synchronized charging and discharging behavior.

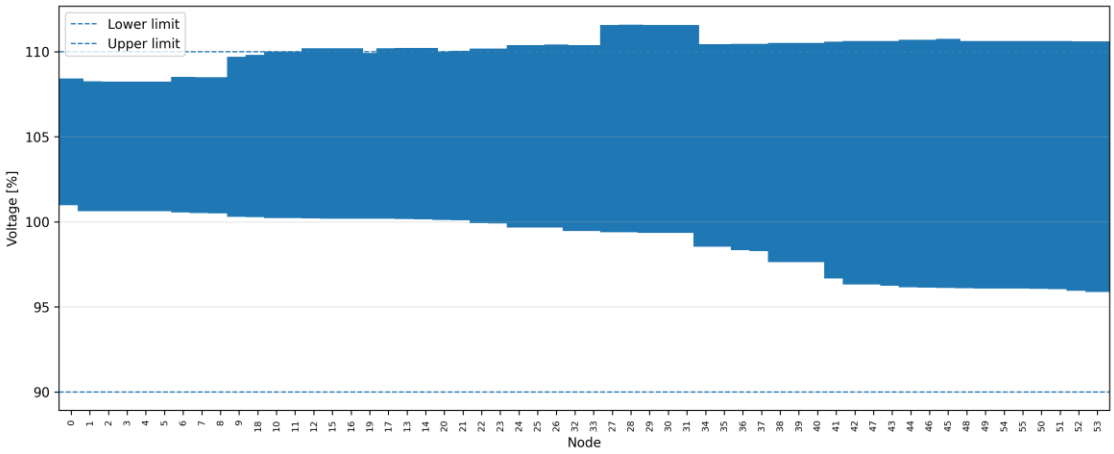


Figure 19 – Voltage range per node for Scenario 5

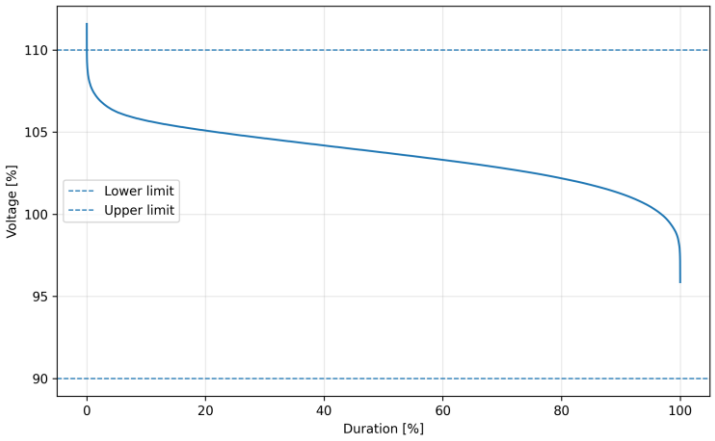


Figure 20 – Voltage duration curve for Scenario 5

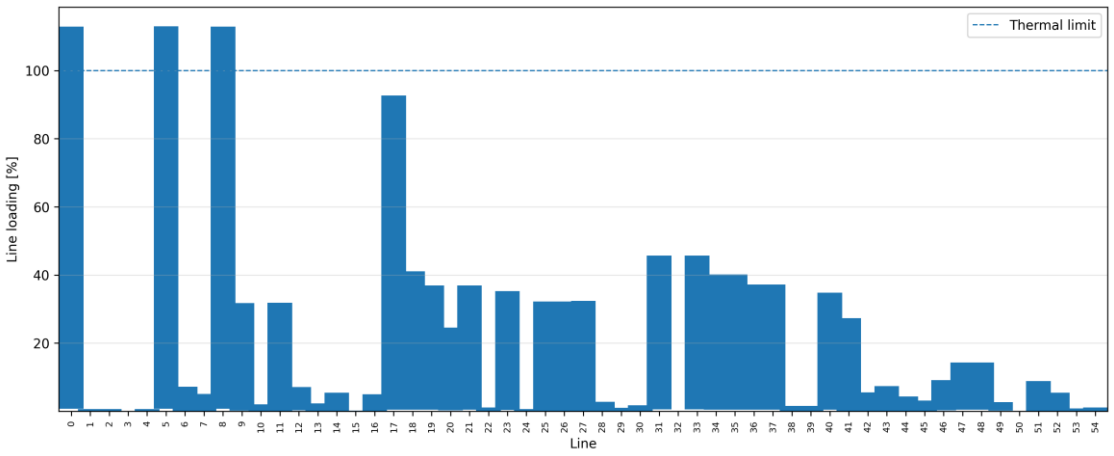


Figure 21 – Line loading range per line for Scenario 5

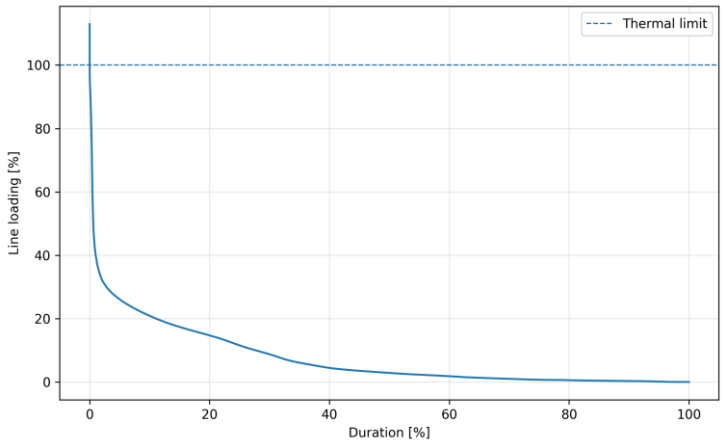


Figure 22 – Line loading duration curve for Scenario 5

Tabela VI – Statistics for Scenario 5

Metric	Value	Critical elements
Minimum voltage [%]	95.866	53
Maximum voltage [%]	111.5898	28
Maximum line loading [%]	112.9342	5
Nodes with undervoltage	/	/
Nodes with overvoltage	44	11-55
Lines with overload	3	0, 5, 8
Total hours below voltage limit [h]	/	/
Total hours above voltage limit [h]	42.5	/
Total hours above loading limit [h]	15.75	/
Annual active energy losses [MWh]	200.35	/

Results from Scenario 6

Figures 23–26 and Table VII present the results for Scenario 6, representing the most critical operating condition analyzed in this study. In this scenario, the network operates at the HC limit while the BESS units are additionally allowed to charge from the grid. As shown in Figure 23 and summarized in Table VII, the maximum voltage remains at 111.59%, while the minimum voltage decreases to 92.67% at node 53. The voltage duration curve presented in Figure 24 shows that overvoltage conditions occur for 388.5 hours during the analyzed year, affecting 46 nodes. Simultaneously, Figure 25 demonstrates a substantial increase in line loading, with the maximum loading reaching 174.38% on line 1. According to Figure 26 and Table VII, four lines experience thermal overloads, with a cumulative overload duration exceeding 4166 hours annually. Furthermore, the annual active energy losses increase dramatically to 510.86 MWh, representing more than a threefold increase compared to Scenario 1. These results clearly demonstrate that unrestricted market-driven charging of BESS units under high PV penetration conditions can introduce severe operational problems in the DN, primarily due to the synchronized charging behavior of multiple storage systems during low-price periods.

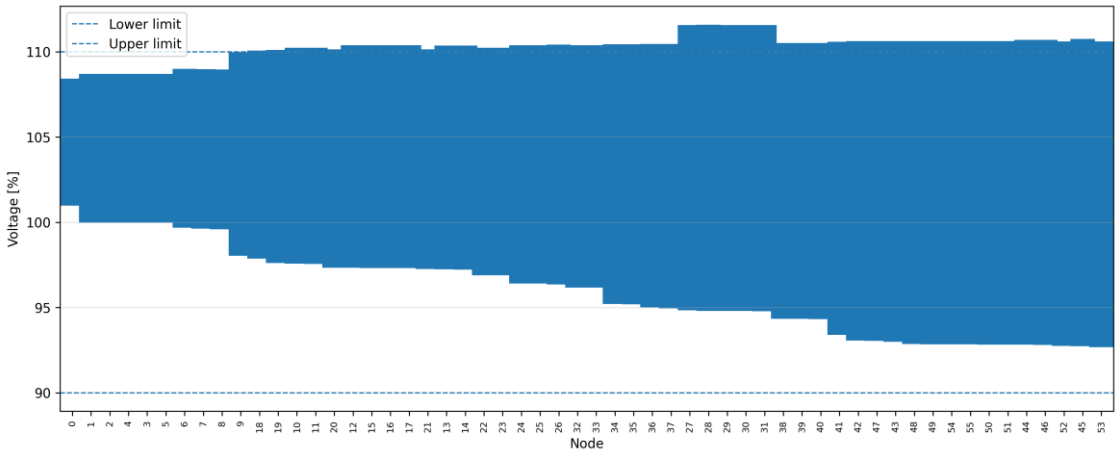


Figure 23 – Voltage range per node for Scenario 6

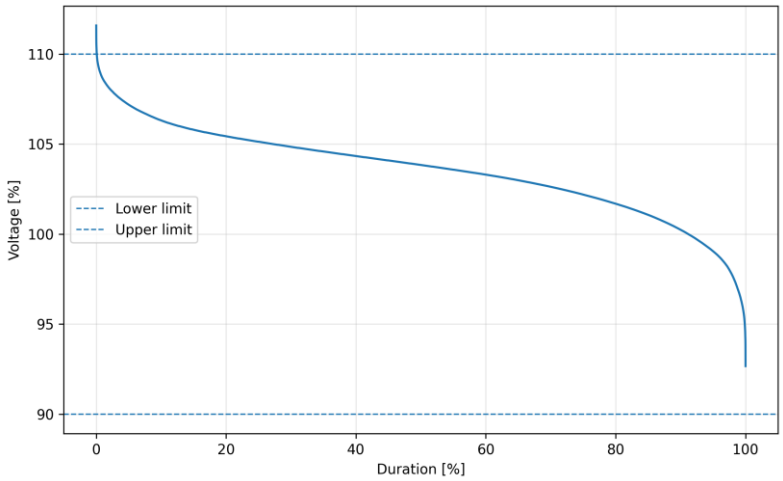


Figure 24 – Voltage duration curve for Scenario 6

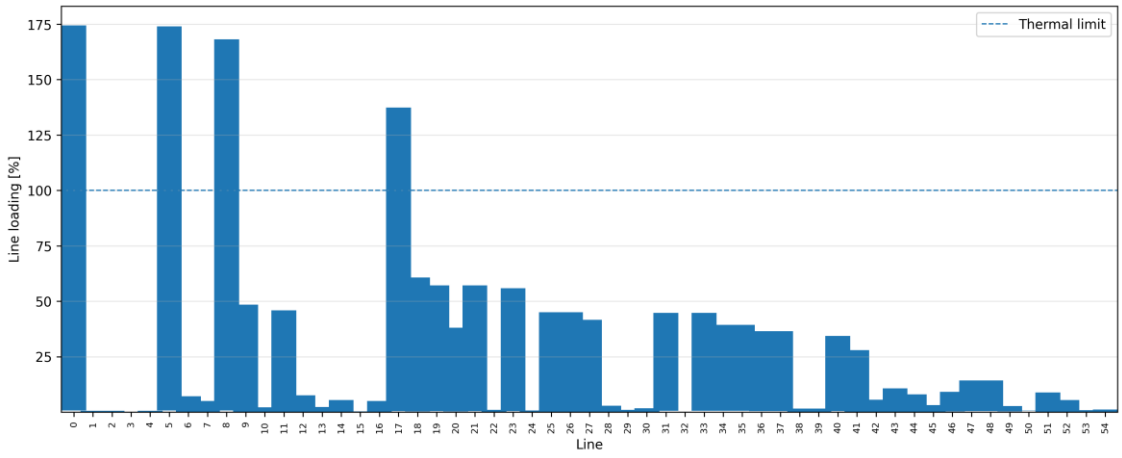


Figure 25 – Line loading range per line for Scenario 6

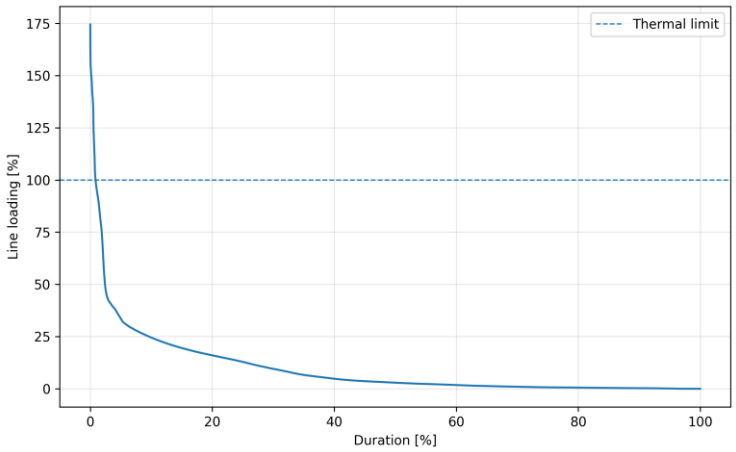


Figure 26 – Line loading duration curve for Scenario 6

Tabela VII – Statistics for Scenario 6

Metric	Value	Critical elements
Minimum voltage [%]	92.6679	53
Maximum voltage [%]	111.5898	28
Maximum line loading [%]	174.3793	1
Nodes with undervoltage	/	/
Nodes with overvoltage	46	9 - 55
Lines with overload	4	0, 5, 8, 17
Total hours below voltage limit [h]	/	/
Total hours above voltage limit [h]	388.5	/
Total hours above loading limit [h]	4166.75	/
Annual active energy losses [MWh]	510.86	/

The obtained results demonstrate a clear trade-off between the economic operation of BESS under energy arbitrage strategies and the secure operation of the DN. While BESS integration can improve the economic performance of PV systems, unrestricted charging from the grid significantly increases network stress, particularly under high PV penetration levels. The results further show that the temporal synchronization of charging and discharging actions plays a critical role in the occurrence of voltage and thermal constraint violations

4. CONCLUSION

The obtained results demonstrate that the impact of PV–BESS systems on DN operation strongly depends on the charging strategy of the batteries and the PV penetration level. Under the existing PV penetration level, the integration of BESS introduces only limited impacts on voltage profiles, line loading, and network losses. However, when the PV penetration is increased up to the hosting capacity limit, the operation of BESS begins to introduce noticeable operational challenges. When the BESS units are restricted to charging only from local PV generation, the resulting overvoltages and line overloads remain relatively limited both in magnitude and duration. The overvoltage conditions occur for short time intervals, typically not exceeding one hour per day, indicating that such disturbances could potentially be mitigated

through demand-side management programs, local flexibility activation, or minor operational adjustments, without requiring significant network reinforcements. On the other hand, allowing BESS charging from the grid can substantially increase network stress under high PV penetration conditions. In this case, the duration and severity of voltage and thermal constraint violations increase significantly due to the synchronized charging behavior of multiple BESS units during low-price periods. The obtained results indicate that under such operating conditions, conventional operational measures are unlikely to be sufficient, and strengthening of the DN infrastructure, including line and transformer upgrades, would likely be required to ensure secure network operation. Overall, the results highlight the importance of explicitly considering DN constraints in the operation and planning of arbitrage-driven PV–BESS systems.

LITERATURE

[1] López Prol, J., Steininger, K.W., Zilberman, D. — "The cannibalization effect of wind and solar in the California wholesale electricity market," *Energy Economics*, vol. 85, 2020.
[2] Peña, J.I., Rodríguez, R., Mayoral, S. — "Cannibalization, depredation, and market remuneration of power plants," *Energy Policy*, vol. 167, 2022.
[3] Reichenberg, L., Ekholm, T., Boomsma, T. — "Revenue and risk of variable renewable electricity investment: The cannibalization effect under high market penetration," *Energy*, vol. 284, 2023.
[4] Garcia, J.L. et al. — "Impact of Electricity Price Reductions on the Profitability and Sizing of Photovoltaic Systems in Agri-Food Industries," *Agronomy*, vol. 15, 2025.
[5] Oudalov, A., Pusceddu, E., Zakeri, B., Castagneto Gissey, G. — "Synergies between energy arbitrage and fast frequency response for battery energy storage systems," *Applied Energy*, vol. 283, 2021
[6] Saldarini, A. et al. — "Profitability of energy arbitrage net profit for grid-scale BESS considering dynamic efficiency and degradation," *Journal of Energy Storage*, 2024.
[7] Uddin, M. et al. — cited in: Chand, A. et al., "A review of battery energy storage systems for ancillary services in distribution grids," *Frontiers in Energy Research*, vol. 10, 2022.
[8] Ma, Y. et al. — "A Novel Probabilistic Framework to Study the Impact of PV-Battery Systems on Low-Voltage Distribution Networks," *IEEE Transactions on Power Systems*, 2019.
[9] de Carvalho, W., Attarha, A., Pota, H.R. — "Optimization-Based Control of Distributed Battery Storage in Distribution Networks," *IEEE*, 2024
[10] Pompern, N. et al. — "Optimal placement and capacity of battery energy storage system in distribution networks integrated with PV and EVs," *IEEE Access*, 2023.
[11] Cutler, D. et al. — "Coordinating distributed energy resources for reliability can significantly reduce future distribution grid upgrades and peak load," *Joule*, vol. 7, 2023.
[12] Pamshetti, V.B. et al. — "Enhanced Battery Degradation-Aware Scheduling for Distribution Network with Electric Vehicle Load," 2024 (arXiv:2407.06857).
[13] Barla, M.C., Sarkar, D. — "Optimal placement and sizing of BESS in RES-connected distribution network," *Int. J. Systems Assurance Engineering*, 2023.
[14] G. Veljanovski, P. Popovski, M. Atanasovski, K. Bilbiloska and A. K. Mateska, "Impact of Load Flexibility on Photovoltaic Hosting Capacity in Distribution Networks," 2024 *20th International Conference on the European Energy Market (EEM)*, Istanbul, Turkiye, 2024, pp. 1-5, doi: 10.1109/EEM60825.2024.10608894.
[15] IBM ILOG CPLEX (2026). *V[12.9]: User's Manual for CPLEX*. International Business Machines Corporation.
[16] Python Software Foundation, "Python Language Reference, version 3.9"
[17] L. Thurner, A. Scheidler, F. Schäfer, J.-H. Menke, J. Dollichon, F. Meier, S. Meinecke, and M. Braun, "pandapower—An Open-Source Python Tool for Convenient Modeling, Analysis, and Optimization of Electric Power Systems," *IEEE Transactions on Power Systems*, vol. 33, no. 6, pp. 6510–6521, Nov. 2018.
[18] HUPX Hungarian Power Exchange, "HUPX Day-Ahead Market"